DOI: 10.1002/ejic.200501098

Synthesis, Structure, and Magnetic Behavior of Two New 1D Polymeric Manganese Azido Complexes

Morsy A. M. Abu-Youssef,*[a] Albert Escuer,[b] and Vratislav Langer[c]

Keywords: Manganese / Coordination polymers / Azido complexes / Aqua complexes / Magnetic properties

Two new Mn^{II} one-dimensional compounds with formulae $[Mn(\mu\text{-}N_3)_2(pyzamid)_2]_n$ (**1**) and $[Mn_2(3\text{-}ampy)_4(\mu\text{-}N_3)_2(N_3)_2(H_2O)_2]_n$, (**2**) (pyzamid = pyrazineamide and 3-ampy = 3-aminopyridine) were structurally and magnetically characterized. Compound **1** crystallizes in the monoclinic system, *P*2/*c* space group, and polymerizes through double end-on azido bridges giving 1D chains with the Mn^{II} atoms in a MnN_6 environment. Compound **2** crystallizes in the triclinic system, $P\bar{1}$ space group, and consists of alternate $[Mn(3\text{-}ampy)_2(\mu\text{-}N_3)_2(N_3)_2]$ and $[Mn(3\text{-}ampy)_2(\mu\text{-}N_3)_2(H_2O)_2]$ octahedrons (MnN_6 – MnN_4O_2 environments), linked by single end-to-end azido bridges. Both chains show very uncommon topologies. Attemps to obtain manganese/azido derivatives with the qux = quinoline-4-carboxylato anion gave the recently reported compound $[Mn(\mu\text{-}qux)_2(\mu\text{-}H_2O)]_n$ (**3**), which consists of a chain with only carboxylato and aqua bridges with the Mn^{II} atoms in a MnO_6 slightly distorted octahedron. In good agreement with the expected behavior, magnetic susceptibility measurements show weak ferromagnetic interactions for **1**, whereas compound **2** exhibits moderate antiferromagnetic coupling.

Introduction

The flexidentate azide ion has been demonstrated as not only an extremely versatile ligand but also an excellent magnetic mediator, which provides complexes of great structural variety with interesting physical properties.[1–4] The versatility of this ligand is a direct consequence of its ability to link transition metal cations in $\mu\text{-}_{1,1}$ (end-on, EO), $\mu\text{-}_{1,3}$ (end-to-end, EE), $\mu\text{-}_{1,1,3}$, $\mu\text{-}_{1,1,1}$, or still other modes, easily yielding polynuclear, one-, two-, or three-dimensional species with specific topologies.[5–8] The simultaneous presence of more than one of these coordination modes in the same compound, increasing the connectivity possibilities, is not rare.[9] The interest of the magnetochemists in this ligand lies in the well-established relationship between the coordination mode and the resulting magnetic properties, which covers a wide range of ferro-, ferri-, and antiferromagnetic responses.[1] It should be pointed out that the topology of the resulting systems is far from under control because of the similar stabilities of the different coordination modes, which permit other factors such as packing forces or weak supramolecular interactions to be determinant.[10] One of the most complete series of compounds reported to date, with the general formula $[Mn(N_3)_2(R\text{-}py)_2]_n$ (R-py, substituted pyridyl ligands), is a good example of how minor differences in R can drastically change the dimensionality or the coordination mode of the azido bridges, generally because of weak effects such as hydrogen bonds, steric hindrance, or supramolecular π-π stacking interactions in the solid state. As part of our investigation on metal-azido derivatives, we have recently reported a number of transition metal coordination polymers with bidentate or tetradentate neutral organic ligands to built coordination supramolecular frameworks.[8–10]

In this paper we have studied the reaction of azido ligands with Mn^{II} and several polytopic ligands such as the coligands pyzamid = pyrazineamide, 3-ampy = 3-aminopyridine, and qux = quinoline-4-carboxylato anion. These coligands, with almost one aromatic N donor, closely related with previously reported systems such as pyrimidine,[8b] nicotinate anion,[10b] 2-acetylpyridine,[10a,10e] or the same 3-aminopyridine,[10f] were chosen in order to combine the azido versatility with the possibility of a second bridging donor group such as the N pyrazinic or the amide in pyzamid, the amino function in 3-ampy or the carboxylate in qux, in a trial experiment to obtain new topologies. As a result, we present the synthesis, X-ray, and magnetic char-

---

[a] Chemistry Department, Faculty of Science, Alexandria University,
P. O. Box 426, Ibrahimia, 21321 Alexandria, Egypt
Fax: +2-03-3911794
E-mail: morsy5@link.net
[b] Departament de Química Inorgànica and Institut de Nanociència i Nanotecnologia de la Universitat de Barcelona (UN^2UB),
Martí I Franqués 1–11, 08028 Barcelona, Spain
Fax: +34-934907725
E-mail: albert.escuer@qi.ub.es
[c] Environmental Inorganic Chemistry, Department of Chemical and Biological Engineering, Chalmers University of Technology,
41296 Göteborg, Sweden
Fax: +46-31-7722853
E-mail: langer@chalmers.se

acterization of two new polymeric manganese azido derivatives with the formula $[Mn(\mu\text{-}N_3)_2(pyzamid)_2]_n$ (**1**) and $[Mn_2(3\text{-}ampy)_4(\mu\text{-}N_3)_2(N_3)_2(H_2O)_2]_n$ (**2**). For compound **1** the pyrazineamide ligand coordinates through only one of its donor N atoms in a similar way to a classical pyridine ligand. In this case double EO azido bridges provide the second example[8a] of an EO-azido one-dimensional system. Compound **2** also has monodentate 3-aminopyridine ligands such as in $[Mn(3\text{-}ampy)_4(N_3)_2]$[10f] but the topology of the resulting system is very uncommon: alternating $[Mn(3\text{-}ampy)_2(\mu\text{-}N_3)_2\ (N_3)_2]$ and $[Mn(3\text{-}ampy)_2(\mu\text{-}N_3)_2(H_2O)_2]$ coordination polyhedra, linked by single EE azido groups gives the 1D arrangement. The reaction with the qux ligand gave the very recently reported compound $[Mn(\mu\text{-}qux)_2(\mu\text{-}H_2O)]_n$ (**3**).[11] In this case the qux ligand only coordinates by means of the carboxylato groups while azido groups do not coordinate to the manganese atoms. The structure of **3** is closely related to the similar $[Cd(qux)_2(H_2O)]_n$ complex.[12] The magnetic response agrees with the expected properties for the different kinds of bridges, that is to say, weak ferromagnetic interactions for the 1D EO-azido chain **1** and moderately weak antiferromagnetic coupling for the EE-azido chain **2**. Compound **3** shows weak antiferromagnetic coupling as was reported.[11]

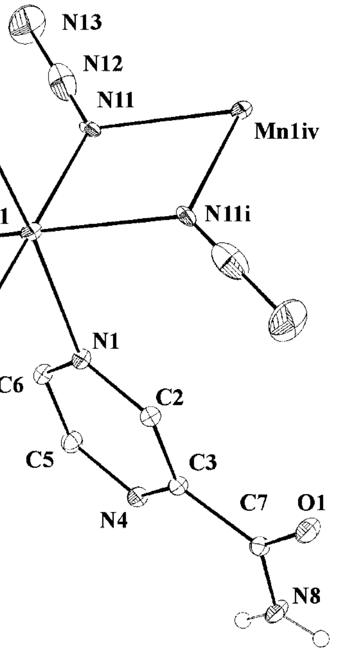

Figure 1. Numbering scheme for $[Mn(\mu\text{-}N_3)_2(pyzamid)_2]_n$ (**1**) with atomic displacement parameters shown at the 30% probability level. Symmetry codes are given in Table 1.

Results and Discussion

Structure of $[Mn(\mu\text{-}N_3)_2(pyzamid)_2]_n$ (1)

A labeled ORTEP plot of the structure is shown in Figure 1. Selected distances and angles are listed in Table 1.

The structure consists of neutral 1D chains of Mn^{II} cations linked by double end-to-end azido bridges, along the *b* axis, see Figure 2. The manganese ions, positioned on twofold axes, are placed in a distorted octahedral geometry, MnN_6, linked to four bridging azides in the equatorial plane and two terminal *trans* pyzamid-groups in the apical positions. Mn–N(azido) and Mn–N(pyrazine) bond lengths are very similar lying in the range 2.328(3)–2.349(3) Å. The four-membered ring $Mn1–N11–Mn1^{iv}–N11^{i}$ is fully planar with Mn–N–Mn bond angles of 97.1(1)°. The Mn···Mn distance is 3.510(1) Å along the chain in the *b* direction. Aromatic rings coordinated at the *trans* sites to the manganese atoms shows a distance between the centroids of 3.510 Å, as result of the short Mn···Mn distances through the double end-on bridges, Figure 2.

The structure is stabilized in the (*a*,*c*) plane by hydrogen bonds involving the N4 atoms from the pyrazine ligands, as well as the N8 and O1 from the amide function, Table 2. The strongest interchain H bonds corresponds to N8–H···O1 [donor–acceptor distance is 2.907(4) Å with a hy-

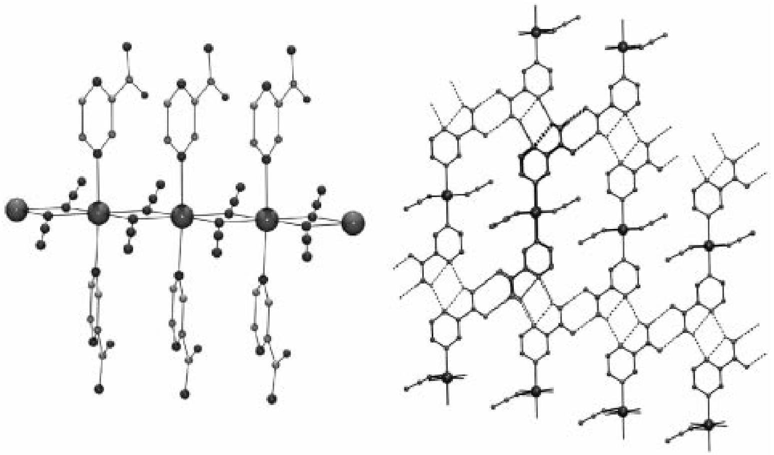

Figure 2. Left, view along the *c*-axis of the one-dimensional compound **1**, showing the double end-on azido bridges between the manganese atoms and the parallel arrangement of the pyrazine rings along the chain in the *b*-direction. Right, view of the structure of **1** projected along the *b*-direction, showing the intra and interchain H-bond network. H bonds involve the N4 atom from the pyrazine ring, O1 from the amide function, and N8 ($–NH_2$) from the same function.

Table 1. Selected bond lengths [Å] and bond angles [°] for complex $[Mn(\mu\text{-}N_3)_2(pyzamid)_2]_n$ (**1**).

Mn1–N1^{i}	2.328(3)	N1–Mn1–N11	92.7(1)
Mn1–N1	2.328(3)	N11^{i}–Mn1–N11	83.2(2)
Mn1–N11^{i}	2.332(3)	N1^{i}–Mn1–N11^{ii}	87.3(1)
Mn1–N11	2.332(3)	N1–Mn1–N11^{ii}	89.5(1)
Mn1–N11^{ii}	2.349(3)	N11^{i}–Mn1–N11^{ii}	179.6(1)
Mn1–N11^{iii}	2.349(3)	N11–Mn1–N11^{ii}	97.1(1)
		N1^{i}–Mn1–N11^{iii}	89.5(1)
N11–N12	0.960(5)	N1–Mn1–N11^{iii}	87.3(1)
N12–N13	1.236(6)	N11^{i}–Mn1–N11^{iii}	97.1(1)
		N11–Mn1–N11^{iii}	179.6(1)
N1^{i}–Mn1–N1	175.8(1)	N11^{ii}–Mn1–N11^{iii}	82.5(2)
N1^{i}–Mn1–N11^{i}	92.7(1)		
N1–Mn1–N11^{i}	90.5(1)	Mn1–N11–Mn1^{iv}	97.1(1)
N1^{i}–Mn1–N11	90.5(1)	N12–N11–Mn1^{iv}	121.5(3)
		N11–N12–N13	178.9(6)

Symmetry transformations used to generate equivalent atoms: (i): $-x+1, y, -z+1/2$; (ii): $x, y-1, z$; (iii): $-x+1, y-1, -z+1/2$; (iv): $x, y+1, z$

drogen bond angle of 180(6)°], weaker H bonds correspond to the bifurcated N8···N4 [donor–acceptor distances 2.762(4) and 3.112(4) Å, with hydrogen bond angles of 103(4)° and 146(4)°, respectively], see Figure 2, whereas weak intrachain contacts are given by the bifurcated interaction C6–H···N13. Coordination as a monodentate ligand of the pyrazine ring can be justified by two reasons: the steric hindrance of the amide group, too close to N4, and the additional stabilization of the structure provided by the H-bond network.

Table 2. H-Bond parameters for compounds **1** and **2**.

D–H···A	d(D–H) [Å]	d(H···A) [Å]	d(D···A) [Å]	∠(D–H···A) [°]
Compound **1**				
N8–H8A···O1^{v}	0.77(5)	2.14(5)	2.907(4)	180(6)
N8–H8B···N4	0.84(5)	2.45(5)	2.762(4)	103(4)
N8–H8B···N4^{vi}	0.84(5)	2.38(5)	3.112(4)	146(4)
C6–H6···N13^{vii}	0.95	2.44	3.248(6)	143
C6–H6···N13^{viii}	0.95	2.60	3.072(5)	111
Symmetry transformations used to generate equivalent atoms: (v): $-x+2, -y+1, -z+1$; (vi): $-x+2, y, -z+1/2$; (vii): $-x+1, -y, -z$; (viii): $-x+1, -y+1, -z$				
Compound **2**				
O1–H1A···N23^{iii}	0.88(3)	1.93(3)	2.805(3)	172(3)
O1–H1B···N3A^{iv}	0.82(3)	2.04(3)	2.856(3)	178(3)
N13–H13A···N3A^{iv}	0.89(3)	2.37(3)	3.238(3)	167(2)
N13–H13B···N3B^{iii}	0.82(3)	2.44(3)	3.242(3)	163(2)
N23–H23A···O1^{v}	0.92(3)	2.28(3)	3.167(3)	161(2)
N23–H23B···N13^{ii}	0.95(3)	2.23(3)	3.171(3)	174(2)
C12–H12···N3A^{iv}	0.95	2.62	3.444(3)	146
C14–H14···N2A^{iii}	0.95	2.58	3.407(3)	146
C24–H24···N1B^{vi}	0.95	2.56	3.282(3)	132

Symmetry transformations used to generate equivalent atoms: (iii): $x-1, y+1, z$; (iv): $x-1, y, z$; (v): $-x, -y, -z$; (vi): $x, y-1, z$

Structure of $[Mn_2(3\text{-ampy})_4(\mu\text{-}N_3)_2(N_3)_2(H_2O)_2]_n$ (2)

A labeled ORTEP plot of the structure is shown in Figure 3. Selected distances and angles are listed in Table 3. The structure consists of neutral 1D chains of Mn^{II} along the *a* axis, in which the coordination environment around the manganese atoms shows a regular alternating chain (Figure 4).

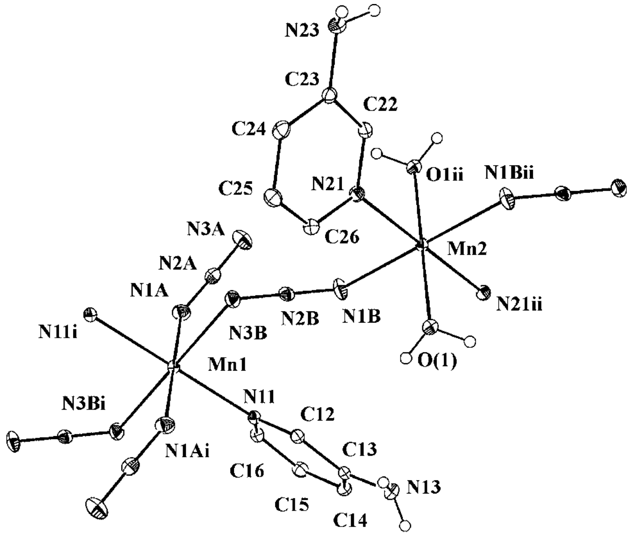

Figure 3. Numbering scheme for $[Mn_2(3\text{-ampy})_4(\mu\text{-}N_3)_2(N_3)_2(H_2O)_2]_n$ (**2**). Atomic displacement parameters are shown at the 30% probability level. Symmetry codes are given in Table 3.

Table 3. Selected bond lengths [Å] and bond angles [°] for complex $[Mn_2(3\text{-ampy})_4(\mu\text{-}N_3)_2(N_3)_2(H_2O)_2]_n$ (**2**).

Bond lengths			
Mn1–N1A^{i}	2.216(2)	Mn2–N1B^{ii}	2.198(2)
Mn1–N1A	2.216(2)	Mn2–N1B	2.198(2)
Mn1–N11	2.251(2)	Mn2–O1^{ii}	2.229(2)
Mn1–N11^{i}	2.251(2)	Mn2–O1	2.229(2)
Mn1–N3B	2.278(2)	Mn2–N21^{ii}	2.242(2)
Mn1–N3B^{i}	2.278(2)	Mn2–N21	2.242(2)
N1A–N2A	1.183(3)	N1B–N2B	1.177(3)
N2A–N3A	1.176(3)	N2B–N3B	1.180(3)
Bond angles			
N1A^{i}–Mn1–N1A	180.0	N1B^{ii}–Mn2–N1B	180.0
N1A^{i}–Mn1–N11	90.88(7)	N1B^{ii}–Mn2–O1^{ii}	88.81(8)
N1A–Mn1–N11	89.12(7)	N1B–Mn2–O1^{ii}	91.19(8)
N1A^{i}–Mn1–N11^{i}	89.12(7)	N1B^{ii}–Mn2–O1	91.19(8)
N1A–Mn1–N11^{i}	90.88(7)	N1B–Mn2–O1	88.81(8)
N11–Mn1–N11^{i}	180.0	O1^{ii}–Mn2–O1	180.0
N1A^{i}–Mn1–N3B	89.59(8)	N1B^{ii}–Mn2–N21^{ii}	88.75(7)
N1A–Mn1–N3B	90.41(8)	N1B–Mn2–N21^{ii}	91.25(7)
N11–Mn1–N3B	91.20(7)	O1^{ii}–Mn2–N21^{ii}	89.85(7)
N11^{i}–Mn1–N3B	88.80(7)	O1–Mn2–N21^{ii}	90.15(7)
N1A^{i}–Mn1–N3B^{i}	90.41(8)	N1B^{ii}–Mn2–N21	91.25(7)
N1A–Mn1–N3B^{i}	89.59(8)	N1B–Mn2–N21	88.75(7)
N11–Mn1–N3B^{i}	88.80(7)	O1^{ii}–Mn2–N21	90.15(7)
N11^{i}–Mn1–N3B^{i}	91.20(7)	O1–Mn2–N21	89.85(7)
N3B–Mn1–N3B^{i}	180.0	N21^{ii}–Mn2–N21	180.0
N2A–N1A–Mn1	134.7(2)	N2B–N1B–Mn2	143.5(2)
N2B–N3B–Mn1	129.9(2)	N1B–N2B–N3B	179.5(2)
N1A–N2A–N3A	177.8(3)		

Symmetry transformations used to generate equivalent atoms: (i): $-x, -y+1, -z+1$; (ii): $-x, -y+1, -z$

There are two independent manganese ions, both positioned on inversion centers giving the alternating chain. The Mn1 ion is placed in a slightly distorted octahedral geome-

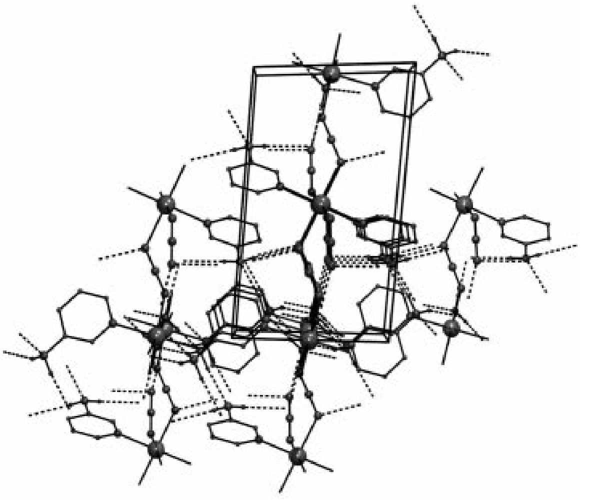

Figure 4. View of the one-dimensional compound **2** showing the interchain H bridges involving terminal azido ligands and the $-NH_2$ functions.

try, MnN_6. The equatorial plane is defined by two end-to-end μ-bridging azides and two terminal azides, and the axial sites are occupied by two terminal 3-ampy groups in a *trans* arrangement. The Mn1–N1A bond length (terminal azido ligand) is slightly shorter than the Mn1–N (bridging azido or 3-ampy) distances. The Mn2 ion is placed in a slightly distorted MnN_4O_2 octahedral environment with two end-to-end μ-bridging azides, two 3-ampy ligands in the equatorial plane, and two water molecules in the apical positions. The end-to-end azido bridge gives two slightly different bond angles with the manganese atoms, Mn1–N3B–N2B of 129.9(2)° and Mn2–N1B–N2B of 143.5(2)°, and a Mn–N–N–N–Mn dihedral angle of 165.1°.

The Mn1···Mn2 distance is 6.3507(2) Å along the chains, whereas the minimum interchain distance is equal to 7.8105(2) Å.

The structure is stabilized by a large number of strong hydrogen bonds that involve O1 from the water molecules, N13 and N23 from the amino functions, the terminal azido atoms N3A, and also one of the atoms of the bridging azido group, N3B, Table 2. One of them is an intrachain contact between the aminated groups N23–H23B···N13^{ii} whereas the other contacts, involving the water molecules and the azido ligands, are all interchain contacts, Figure 4. This H-bond network gives a 3D supramolecular arrangement as occurs in compound **1**. The aromatic rings of neighbor chains interact between them by means of π-π interactions with distances between centroids of 3.394 and 3.510 Å.

Structure of $[Mn(\mu\text{-qux})_2(\mu\text{-}H_2O)]_n$ (3)

A schematic plot of the structure of **3** is shown in Figure 5. The structure of this compound can be described as 1D chains of manganese atoms along the *c* axis, linked by two *syn-syn* carboxylates and one $\mu\text{-}OH_2$ molecule. The manganese ions, positioned on inverse centers, are placed in a slightly distorted octahedral geometry, MnO_6, linked to four bridging quinoline-4-carboxylato ligands and two axial O atoms from bridging water molecules. The Mn^{II}–O(carboxylate) bond lengths lie in the range 2.103(2)–2.171(2) Å and they are shorter than the Mn^{II}–O(water) distances, 2.286(2) Å. The bond angle Mn–O(water)–Mn′ has a value of 114.1(2)°.

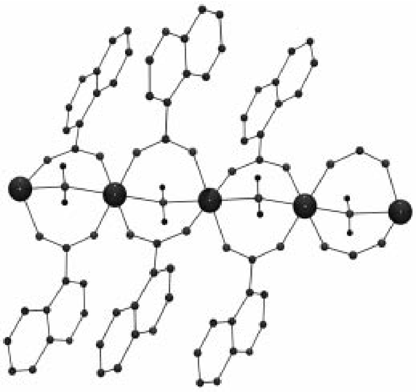

Figure 5. Schematic view of $[Mn(\mu\text{-qux})(\mu_2\text{-}H_2O)]_n$ (**3**).

The structure is stabilized in the (*a*,*b*) plane by strong interchain $O_{water}\cdots N_{quinoline}$ hydrogen bonds [donor–acceptor distance is 2.742(3) Å with a hydrogen-bond angle of 179(4)°]. Each water molecule participates in two H bonds with *N*-quinoline atoms from two different chains. The aromatic rings from neighboring chains show π-π stacking with interplanar distances of 3.381(3) Å.

Synthetic and Structural Features

Polymeric systems with exclusively end-on azido bridges, all of them characterized by Mn^{II} cations, are very uncommon and only three related compounds have been reported to date. One of them is also a one-dimensional compound with the formula $[Mn(N_3)_2(2\text{-bzpy})]_n$, 2-bzpy = 2-benzoylpyridine, which stabilizes the system by means of interchain π-π stacking of the aromatic rings.[8a]

The other two are bidimensional systems in which the one-dimensional manganese-azido chains are linked between them by means of a second bridging coligand such as bis-monodentate pyrazine[5d] (pyz) or the bis-bidentate 2,2′-bipyrimidine (bpym).[13] The compound $[Mn(N_3)_2(pyz)]_n$ also shows an extensive π-π stacking of parallel pyrazine rings (distance between the rings is 3.412 Å), which contributes to stabilize the structure, Scheme 1.

Less clear are the factors that stabilize the other compound, with formula $[Mn_2(N_3)_4(bpym)]_n$, for which π-π stacking or H bonds cannot be found, but this case is not totally comparable because the coligand is bis-bidentate. In our case, compound **1** exhibits the same kind of interaction between the aromatic rings, which seems to be a quasi general factor that favors these types of compounds.

The variety of compounds that can be obtained with other pyrazines or the 3-ampy ligand are much more difficult to rationalize. As is shown in Scheme 1, nonsubstituted

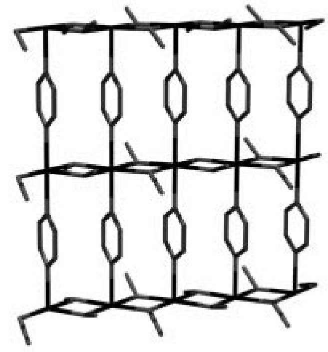

Scheme 1.

pyrazine is able to coordinate both nitrogen atoms but steric hindrance in substituted pyrazines prevents this kind of coordination and only one of the N ring atoms can act as a donor. If the function attached to the pyrazine ring contains coordinating groups, the ligand can act as bidentate, as occurs with pyrazinecarbozylate[14a] and methyl-imidopyrazinecarboxylate,[14b] which gives high-dimensional compounds in both cases. In our case, compound **1**, pyrazineamide coordinates by only one N-ring donor following the general trend for substituted pyrazines, but the poor coordinating amido functions do not act as donors and are involved in intrachain H bonds.

It should be pointed out that small differences in the synthetic procedure can produce very different compounds as occurs in the case of the ligand 3-ampy: an excess of 3-ampy (ratios of Mn^{II}, 3-ampy, and sodium azide 1:7:2) yield the mononuclear compound $[Mn(3\text{-ampy})_4(N_3)_2]$, which is to be expected from the large 3-ampy concentration.[10f] In contrast, similar ratios 1:2.5:2.5 or 1:2:3 give either the $[Mn_2(3\text{-ampy})_4(\mu_{1,1}\text{-}N_3)_2(\mu_{1,3}\text{-}N_3)(N_3)(H_2O)]_n$ system[15] with alternating coordination modes of the azido bridge or the above described $[Mn_2(3\text{-ampy})_4(\mu_{1,3}\text{-}N_3)_2(N_3)_2(H_2O)_2]_n$ (**2**) with alternating coordination polyhedra. This pair of compounds that differs by only one water molecule in their empirical formula, are a nice example of the similar stability of end-on and end-to-end coordinations for the azido ligand.

Magnetic Measurements and Coupling Constant Calculations

The magnetic measurements were performed on powdered crystalline samples in the 2–300 K temperature range. The shape of the plots indicate that the overall interaction is weakly ferromagnetic for compound **1** and moderately antiferromagnetic for **2** and **3**.

Compound **1** shows a $\chi_M T$ room temperature value of 4.78 $cm^3 \cdot K \cdot mol^{-1}$, greater than the expected value of 4.375 $cm^3 \cdot K \cdot mol^{-1}$ for an isolated manganese atom. χ_M increases continuously on cooling and $\chi_M T$ also increases up to a maximum value of 8.31 $cm^3 \cdot K \cdot mol^{-1}$ at 8 K, decreasing down to 4.5 $cm^3 \cdot K \cdot mol^{-1}$ at 2 K, Figure 6. Fitting the $\chi_M T$ data as a homogeneous $S = 5/2$ chain in the 300–15 K temperature range, applying the analytical expression for a regular chain derived from the Hamiltonian $H = -JS_i \cdot S_{i+1}$ (for local $S = 5/2$),[16] gives the best fit parameters $J = +1.1(1)\ cm^{-1}$, $g = 2.045(3)$. The weak ferromagnetic response is in good agreement with the expected properties. End-on azido bridges with M–N–M bond angles around 100° gives typically ferromagnetic coupling and the J value is similar to that reported for the related compound $[Mn(\mu_{1,1}\text{-}N_3)_2(2\text{-bzpy})_2]_n$ (2-bzpy = 2-benzoylpyridine), previously reported by us,[8a] and also agrees with the calculated values for the ferromagnetic interaction in $[Mn(N_3)_2(pyz)]_n$[5d] and $[Mn_2(N_3)_4(bpym)]_n$.[13] Also, the g value, slightly greater than 2.00, agrees with this previously reported chain.[8a] The only difference for the $[Mn(\mu_{1,1}\text{-}N_3)_2(2\text{-bzpy})_2]_n$ compound lies in the H bonds that afford weak antiferromagnetic interchain interactions at very low temperatures; their effect can be seen in the decrease of $\chi_M T$ below 8 K. As can be expected, magnetization measurements, performed at 2 K, show a fast increase in the magnetization, reaching a value equivalent to five electrons for the manganese atom under moderate external fields, Figure 6.

In contrast, compound **2** shows a different response, with a maximum molar susceptibility at 13 K, Figure 7. On the basis of the structural data, compound **2** is an alternating one-dimensional system, which shows similar bond lengths, quite similar Mn–N–N bond angles, and identical torsion angles in the bridging region. A fit of the system was performed assuming that the two J coupling constants have

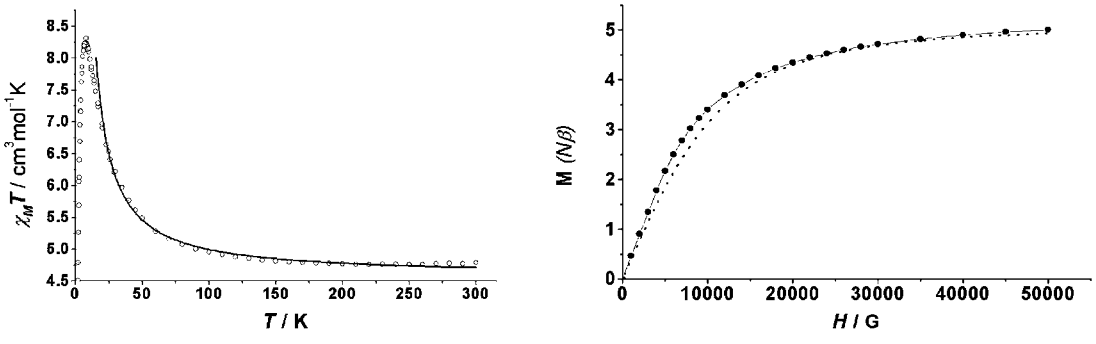

Figure 6. Plot of $\chi_M T$ for compound **1** (left plot). Solid line corresponds to the best fit (see text). Right, magnetization of compound **1**; dotted line shows the Brillouin plot for an uncoupled $S = 5/2$.

the same value under these conditions and by applying the analytical expression for a regular $S = 5/2$ chain; best fit parameters were $J = -3.15(2)\ \mathrm{cm}^{-1}$ and $g = 2.000(5)$. Attempts to differentiate between the two J values by means of the analytical expression for an alternating $S = 5/2$ chain[17] were unsuccessful. For the manganese–azido bridges, theoretical and experimental work on end-to-end coordination modes indicates that the coupling should be antiferromagnetic in all cases and that the large bond or torsion angles in the bridging region always give a lower interaction. Compound **2** shows one large Mn–N–N bond angle (143.5°) and a moderate dihedral angle in the Mn–N–N–N–Mn bridging region. Under these conditions a moderately low coupling can be expected, mainly derived from the large Mn–N–N bond angle.

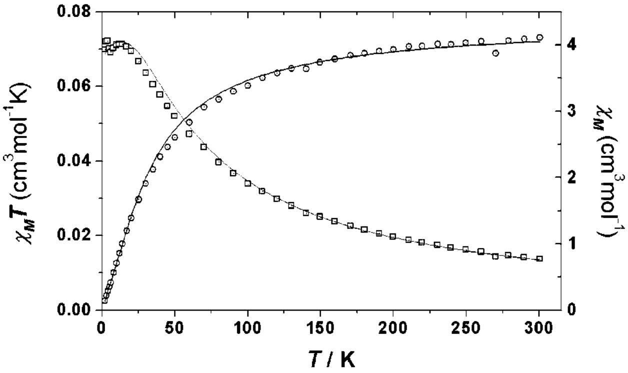

Figure 7. Plot of χ_M (open squares) and $\chi_M T$ (dot centered circles) for compound **2**. Solid line corresponds to the best fit (see text).

Remeasurement of the magnetic properties of compound **3** fully agree with the recently reported[11] data for this compound: molar susceptibility shows a maximum at 17 K, and a fit of the experimental data gives the best fit parameter $J = -2.75(2)\ \mathrm{cm}^{-1}$. This J value agrees with the values reported in the literature for simultaneous carboxylato–aqua bridges, which are always weakly antiferromagnetic.[18]

Conclusions

Two new one-dimensional systems of Mn$^{\mathrm{II}}$ have been obtained and characterized from structural and magnetic points of view. The effect of the coligands employed in the synthesis play a fundamental role in the topology of the final compounds: with 3-pyrazineamide (compound **1**) and 3-aminopyridine (compound **2**) the expected azido chains were obtained but weak packing interactions (π-π stacking and H-bond networks) induce either end-on or end-to-end azido derivatives. In contrast, when the coligand was quinoline-4-carboxylato (compound **3**), the azido ligand did not coordinate to the manganese atoms and one 1D system with *syn-syn* carboxylato and aqua bridges was obtained. Magnetic measurements have been performed for all of them, showing a variety of interactions closely related to the topology of the chains: ferromagnetic interactions for **1**, alternating antiferromagnetic coupling for **2**, and homogeneous antiferromagnetic interactions for **3**.

Experimental Section

General Remarks: Elemental analyses (C,H,N) were carried out using a Perkin–Elmer analyzer, Mn^{2+} was analyzed by a Perkin–Elmer Analyst 300, AAS atomic absorption spectrometer. Infrared spectra (4000–400 cm^{-1}) were recorded with a Bruker IFS-125 model FT-IR spectrophotometer using KBr pellets. Quinoline-4-carboxylic acid, pyrazineamide, and 3-aminopyridine were purchased from Aldrich and other chemicals were of analytical grade quality and used as received. Magnetic susceptibility measurements were carried out on polycrystalline samples with a Quantum Design susceptometer working in the range 20–300 K under magnetic fields of 0.3 T and under a field of 0.03 T in the range 20–2 K at the Magnetochemistry Service of the University of Barcelona. Diamagnetic corrections were estimated from Pascal Tables.

$[\mathrm{Mn}(\mu\text{-}N_3)_2(\mathrm{pyzamid})_2]_n$ (1): A methanolic solution (10.0 mL) of manganese nitrate tetrahydrate (0.5 g, 2 mmol) was mixed with an aqueous/methanolic (1:1) solution (15 mL) of pyrazinamide (0.5 g, ca. 4 mmol). The mixture was stirred for ca. 5 min. A solution of sodium azide (0.65 g, 10 mmol) in water (10 mL) was added dropwise with vigorous stirring. The resulting clear solution was allowed to stand in a refrigerator for several weeks. Colorless needles of the ligand were formed, several days latter yellow needles suitable for X-ray measurements were collected and dried in air with a yield of ca. 45%. $C_{10}H_{10}MnN_{12}O_2$ (385.2): calcd. C 31.18, H 2.62, Mn 14.26, N 43.63; found C 31.0, H 2.5, Mn 14.4, N 43.5. IR (KBr; v: very, s: strong, m: medium, w: weak): $\tilde{\nu}$ = 3393 (s), 3294 (m), 3170 (s), 3091 (s), 2100 (vs), 1718 (vs), 1611 (s), 1590 (s), 1432 (s), 1379 (vs), 1330 (s), 1275 (m), 1187 (m), 1166 (ms), 1100 (m), 1061 (s), 1026 (s), 811 (wm), 787 (ms), 706 (w), 643 (w), 567 (s), 507 (s), 440 (s), 408 (w), 386 (w), 365 (vw), 342 (vw), 315 (vw), 292 (vw), 268 (s) cm^{-1}.

$[\mathrm{Mn}_2(3\text{-ampy})_4(\mu\text{-}N_3)_2(N_3)_2(H_2O)_2]_n$ (2): 3-Aminopyridine (0.19 g, ca. 2 mmol) in methanol (10.0 mL) was added to a solution (10.0 mL) of $\mathrm{MnCl_2}\cdot 4H_2O$ (0.20 g, ca. 1.0 mmol) in methanol. The mixture was stirred for ca. 5 min. Aqueous solutions of sodium azide (0.2 g, 3 mmol) and a few drops of saturated L-ascorbic acid, to prevent oxidation, were added successively and continuously stirred. The resulting clear solution was allowed to stand in a dark place at room temperature for several weeks. Yellowish-brown crystals suitable for X-ray measurements were collected and dried in air with a yield of ca. 65%. $C_{10}H_{14}MnN_{10}O$ (345.2): calcd. C 34.79, H 4.09, Mn 15.91, N 40.57; found C 34.7, H 3.9, Mn 15.9, N 40.5. IR (KBr; v: very, s: strong, m: medium, w: weak, br: broad): $\tilde{\nu}$ = 3343 (vs, br), 3286 (vs, br), 3062 (s), 2631 (m), 2532 (m), 2351 (w), 2310 (w), 2082 (vs), 1661 (s), 1644 (vs), 1605 (vs), 1580 (m), 1488 (vs), 1445 (vs), 1354 (m), 1313 (s), 1277 (s), 1195 (m), 1143 (m), 1096 (m), 1051 (m), 1024 (m), 989 (w), 911 (m), 858 (m), 813 (s), 797 (s), 700 (vs), 644 (s), 610 (s), 594 (s), 477 (m), 407 (m), 388 (m), 343 (w), 315 (w), 292 (w), 268 (s), 232 (s) cm^{-1}.

$[\mathrm{Mn}(\mu\text{-qux})_2(\mu\text{-}H_2O)]_n$ (3): Colorless crystals suitable for X-ray measurements were collected from a 2:1:4 aqueous/methanolic 1:1 solution of quinoline-4-carboxylic acid, manganese nitrate tetrahydrate, and sodium azide. From this mixture that contains a large excess of azido, the neutral chain $[\mathrm{Mn}(\mu\text{-qux})_2(\mu\text{-}H_2O)]_n$, containing only carboxylato bridges, was obtained instead of the expected azido derivative. $C_{20}H_{14}MnN_2O_5$ (417.3): calcd. C 57.57, H 3.38, Mn 13.17, N 6.71; found C 57.4, H 3.3, Mn 13.0, N 6.8. IR (KBr;

Table 4. Crystal data and structure refinement parameters for $[Mn(\mu\text{-}N_3)_2(pyzamid)_2]_n$ (**1**) and $[Mn_2(3\text{-}ampy)_4(\mu\text{-}N_3)_2(N_3)_2(H_2O)_2]_n$ (**2**).

	$[Mn(\mu\text{-}N_3)_2(pyzamid)_2]_n$	$[Mn_2(3\text{-}ampy)_4(\mu\text{-}N_3)_2(N_3)_2(H_2O)_2]_n$
Formula	$C_{10}H_{10}MnN_{12}O_2$	$C_{10}H_{14}MnN_{10}O$
Formula mass [g·mol^{-1}]	385.24	345.25
Crystal system	monoclinic	triclinic
Space group	$P2/c$	$P\bar{1}$
a [Å]	14.1496(3)	7.8105(2)
b [Å]	3.5097(1)	8.3423(2)
c [Å]	14.6946(3)	12.7014(3)
α [deg]	90	78.663(1)
β [deg]	100.393(1)	74.482(1)
γ [deg]	90	63.923(1)
V [Å^3]	717.77(3)	713.26(3)
Z	2	2
T [K]	173(2)	173(2)
λ(Mo-K_α) [Å]	0.71073	0.71073
μ(Mo-K_α) [mm^{-1}]	0.959	0.946
d_{calc} [g·cm^{-3}]	1.782	1.608
Crystal size [mm]	0.30 × 0.08 × 0.02	0.18 × 0.18 × 0.04
Max./min. transmission	0.9811/0.7618	0.9632/0.8482
Θ min./max. [°]	2.82/27.49	1.67/30.47
Reflections collected	8638	11546
Independent reflections/R_{int}	1662/0.0396	4304/0.0613
Data/restraints/parameters	1662/18/122	4304/0/223
R [$I > 2\sigma I$][a]	R_1 = 0.0508, wR_2 = 0.1369	R_1 = 0.0449, wR_2 = 0.0848
Rw [all][b]	R_1 = 0.0574, wR_2 = 0.1415	R_1 = 0.0938, wR_2 = 0.1012

[a] $R(F_o) = \Sigma||F_o| - |F_c|| / \Sigma|F_o|$. [b] $Rw(F_o)^2 = \{\Sigma w[(F_o)^2 - (F_c)^2]^2 / [\Sigma w(F_o)^4]\}^{1/2}$.

v: very, s: strong, m: medium, w: weak, br: broad): $\tilde{\nu}$ = 3439 (m, br,) 2765 (m, br), 2353 (m), 1604 (vs), 1579 (vs), 1506 (ms), 1460 (s), 1427 (vs), 1408 (vs), 1377 (vs), 1302 (s), 1267 (m), 1206 (wm), 1153 (m), 1075 (m), 1026 (m), 995 (m), 961 (m), 874 (ms), 802 (s), 784 (s), 765 (s), 740 (ms), 652 (s), 593 (ms), 532 (wm), 510 (wm), 458 (m), 398 (s), 375 (s), 343 (m), 316 (m), 294 (m), 269 (vs) cm^{-1}.

X-ray Crystallographic Study: All diffraction data were collected using a Siemens SMART CCD diffractometer with Mo-K_α radiation (λ = 0.71073 Å, graphite monochromator). The crystals were cooled to 173(2) K by a flow of nitrogen gas using the LT-2A device. A full sphere of reciprocal lattices were scanned by 0.3° steps in ω with a crystal-to-detector distance of 3.97 cm. Preliminary orientation matrices were obtained from the first frames using the SMART program.[19] The collected frames were integrated using the preliminary orientation matrices, which were updated every 100 frames. Final cell parameters were obtained by refinement on the positions of reflections with $I > 10\sigma(I)$ after integration of all the frames using the SAINT program.[19] The data were empirically corrected for absorptions and other effects using the SADABS program.[20] The structures were solved by direct methods and refined by full-matrix least-squares on all F^2 data using SHELXTL.[21] The non-H atoms were refined anisotropically, while hydrogen atoms were refined isotropically with the use of geometrical restraints. The crystallographic and refinement data are summarized in Table 4. Molecular graphics were prepared using the programs Diamond[22] and ORTEP3.[23] Structural determination for **3** was recently reported[11] but with a lower quality. Our refinement led to the same formula $C_{20}H_{14}MnN_2O_5$ and $C2/c$ space group with the parameters a = 15.0903(7) Å, b = 14.3131(7) Å, c = 7.6708(4) Å, β = 92.513(2)°, V = 1655.2(1) Å^3, Z = 4, R_1 = 0.0484, and wR_2 = 0.0772.

CCDC-291400 to -291402 contain the supplementary crystallographic data for this paper. These data can be obtained free of charge from The Cambridge Crystallographic Data Centre via www.ccdc.cam.ac.uk/data_request/cif.

Acknowledgments

This work was supported by the SIDA (Grants 348-2002-6879 and 348-2004-5473 to M. A. and V. L.) and the CICYT (Grant PB03/0538 to A. E.).

---

[1] J. Ribas, A. Escuer, M. Monfort, R. Vicente, R. Cortés, L. Lezama, T. Rojo, *Coord. Chem. Rev.* **1999**, *193–195*, 1027 and references cited therein.

[2] J. M. Lehn, *Supramolecular Chemistry*, VCH, Weinheim, **1985**.

[3] R. Robin, B. F. Abrahms, R. R. Barten, R. W. Gable, B. F. Huskiness, J. Lieu, *Supramolecular Architecture*, American Chemical Society: Washington, DC, **1992**.

[4] *Molecular Magnetism, a Supramolecular Function* (Ed.: O. Kahn), Kluwer, Dordrecht, **1996**.

[5] a) E. Q. Gao, S. Q. Bai, Z. M. Wang, C. H. Yan, *J. Am. Chem. Soc.* **2003**, *125*, 4984; b) E. Q. Gao, Y. F. Yue, S. Q. Bai, Z. He, C. H. Yan, *J. Am. Chem. Soc.* **2004**, *126*, 1419; c) E. Q. Gao, S. Q. Bai, C. F. Wang, Y. F. Yue, C. H. Yan, *Inorg. Chem.* **2003**, *42*, 8456 and references cited therein; d) J. L. Manson, A. M. Arif, J. S. Miller, *Chem. Commun.* **1999**, 1479.

[6] a) A. Escuer, R. Vicente, M. A. S. Goher, F. A. Mautner, *Inorg. Chem.* **1998**, *37*, 782; b) Z. E. Serna, L. Lezama, M. K. Urtiaga, M. I. Arriortua, M. G. B. Barandika, R. Cortés, T. Rojo, *Angew. Chem. Int. Ed.* **2000**, *39*, 344; c) F. Meyer, P. Kircher, H. Pritzkow, *Chem. Commun.* **2003**, 774; d) G. C. Guo, T. C. W. Mak, *Angew. Chem. Int. Ed. Engl.* **1998**, *37*, 3286.

[7] a) M. A. S. Goher, J. Cano, Y. Journaux, M. A. M. Abu-Youssef, F. A. Mautner, A. Escuer, R. Vicente, *Chem. Eur. J.* **2000**, *6*, 778; b) G. S. Papaefstathiou, S. P. Perlepes, A. Escuer, R. Vicente, M. Font-Bardia, X. Solans, *Angew. Chem. Int. Ed.* **2001**, *40*, 884; c) A. Escuer, R. Vicente, M. A. S. Goher, F. A. Mautner, *Inorg. Chem.* **1998**, *37*, 782.

[8] a) M. A. M. Abu-Youssef, A. Escuer, D. Gatteschi, M. A. S. Goher, F. A. Mautner, R. Vicente, *Inorg. Chem.* **1999**, *38*, 5716; b) A. Escuer, R. Vicente, F. A. Mautner, M. A. S. Goher, M. A. M. Abu-Youssef, *Chem. Commun.* **2002**, 64; c) M. A. M.

Abu-Youssef, M. Drillon, A. Escuer, M. A. S. Goher, F. A. Mautner, R. Vicente, *Inorg. Chem.* **2000**, *39*, 5022.

[9] a) J. Cano, Y. Journaux, M. A. S. Goher, M. A. M. Abu-Youssef, F. A. Mautner, G. J. Reiß, A. Escuer, R. Vicente, *New J. Chem.* **2005**, *29*, 306; b) A. Escuer, F. A. Mautner, M. A. S. Goher, M. A. M. Abu-Youssef, R. Vicente, *Chem. Commun.* **2005**, 605; c) M. A. M. Abu-Youssef, A. Escuer, M. A. S. Goher, F. A. Mautner, G. J. Reiß, R. Vicente, *Angew. Chem. Int. Ed.* **2000**, *39*, 1624.

[10] a) M. A. M. Abu-Youssef, *J. Coord. Chem.* **2005**, *58*, 1377; b) M. A. M. Abu-Youssef, *Polyhedron* **2005**, *24*, 1829; c) F. A. Mautner, C. Gspan, K. Gatterer, M. A. S. Goher, M. A. M. Abu-Youssef, W. Sitte, E. Bucher, *Polyhedron* **2004**, *23*, 1217; d) M. A. S. Goher, A. E. H. Abdou, M. A. M. Abu-Youssef, F. A. Mautner, *Transition Met. Chem.* **2001**, *26*, 39; e) M. A. S. Goher, F. A. Mautner, M. A. M. Abu-Youssef, A. K. Hafez, A. M.-A. Badr, *J. Chem. Soc., Dalton Trans.* **2002**, 3309; f) M. A. S. Goher, A. K. Hafez, M. A. M. Abu-Youssef, A. M. A. Badr, C. Gspan, F. A. Mautner, *Polyhedron* **2004**, *23*, 2349.

[11] X. H. Bu, M. L. Tong, Y. B. Xie, J. R. Li, H. C. Chang, S. Kitagawa, J. Ribas, *Inorg. Chem.* **2005**, *44*, 9837.

[12] Z. F. Chen, P. Zhang, R. G. Xiong, D. J. Liu, X. Z. You, *Inorg. Chem. Commun.* **2002**, *5*, 35.

[13] G. De Munno, M. Julve, G. Viau, F. Lloret, J. Faus, D. Viterbo, *Angew. Chem. Int. Ed. Engl.* **1996**, *35*, 1807; R. Cortés, L. Lezama, J. L. Pizarro, M. I. Arriortua, T. Rojo, *Angew. Chem. Int. Ed. Engl.* **1996**, *35*, 1810.

[14] a) M. A. S. Goher, F. A. Mautner, A. Popitsch, *Polyhedron* **1993**, *12*, 2557; b) E. Q. Gao, Y. F. Yue, S. Q. Bai, Z. He, S. W. Zhang, C. H. Yan, *Chem. Mater.* **2004**, *16*, 1590.

[15] M. A. M. Abu Youssef, A. Escuer, M. A. S. Goher, F. A. Mautner, R. Vicente, *J. Chem. Soc., Dalton Trans.* **2000**, 413.

[16] M. E. Fisher, *Am. J. Phys.* **1964**, *32*, 343.

[17] R. Cortés, M. Drillon, X. Solans, L. Lezama, T. Rojo, *Inorg. Chem.* **1997**, *36*, 677.

[18] a) B. Ye, T. Mak, I. D. Williams, X. Li, *Chem. Commun.* **1997**, 1813; b) I. J. Kim, D. Y. Jung, *Inorg. Chem.* **2000**, *39*, 1470; c) I. J. Kim, E. W. Lee, D. Y. Jung, *Chem. Mater.* **2001**, *13*, 2684; C. Ma, C. Chen, Q. Liu, F. Chen, D. Liao, L. Li, L. Sun, *Eur. J. Inorg. Chem.* **2004**, *43*, 3316.

[19] *SMART & SAINT – Area Detector Control and Integration Software*, Siemens AXS, Madison, WI, USA, **1995**.

[20] G. M. Sheldrick, *SADABS – Program for Empirical Absorption Correction of Area Detectors* (Version 2.03), University of Göttingen, Germany, **2002**.

[21] *SHELXTL – Structure Determination Programs* (Version 6.10), Bruker AXS Inc., Madison, Wisconsin, USA, **2001**.

[22] K. Brandenburg, *Diamond – Visual Crystal Structure Information System* (Version 3.0e), Crystal Impact GbR, Bonn, Germany, **2005**.

[23] *ORTEP3* (Version 1.08): L. J. Farrugia, *J. Appl. Crystallogr.* **1997**, *30*, 565.

Received: December 7, 2005